Food Research International 157 (2022) 111382

Contents lists available at ScienceDirect

Food Research International

journal homepage: www.elsevier.com/locate/foodres

The intestinal colonization of *Lactiplantibacillus plantarum* AR113 is influenced by its mucins and intestinal environment

Wenfei Qin, Yongjun Xia, Zhiqiang Xiong, Xin Song, Lianzhong Ai, Guangqiang Wang *

School of Health Science and Engineering, Shanghai Engineering Research Center of Food Microbiology, University of Shanghai for Science and Technology, Shanghai 200093, China

ARTICLE INFO

Keywords:
L. plantarum
Mucin
Intestinal environment
Colonization

ABSTRACT

Lactiplantibacillus plantarum is an important member of the probiotic family and colonization of the host intestinal is essential for its continued probiotic function. The mechanism of *L. plantarum* intestinal colonization has not been elucidated until now, an important reason being that the colonization process is influenced by a number of factors. In this study, to confirm the influences of adhesion ability and host intestinal environment on *L. plantarum* intestinal colonization, knockouts of *L. plantarum* AR113 mucin genes were constructed using CRISPR/Cas9 gene editing technology, and polyethylene glycol was used to reduce the intestinal flora abundance. The knockout of *L. plantarum* AR113 mucin genes barely altered the strain's tolerance to acid and bile salts. Notably, the adhesion number of AR113Δ*Lp*_1431Δ*Lp*_2233Δ*Lp*_2792 to HT-29 cells was reduced from 175 to 114 per 100 cells. Through in vivo colonization experiments, an increase in the fluorescence intensity of AR113 and AR113Δ*Lp*_1431&2233&2792 was detected the day after the mice were fed, while the deletion of *Lp*_1431, *Lp*_2233 and *Lp*_2792 genes reduced the intestinal tract colonization time from 14 to 11 days. Both AR113 and AR113Δ*Lp*_1431Δ*Lp*_2233Δ*Lp*_2792 were reproduced in the intestine by labeling with 5-(6)-carboxyfluorescein diacetate N-succinimidyl ester. The results showed that the change in fluorescence intensity was closely dependent on the number of adhesions. Finally, compared to the control group, the prolonged intestinal colonization time of AR113Δ*Lp*_1431Δ*Lp*_2233Δ*Lp*_2792 increased mice intestinal flora abundance, with distributions in the duodenum, jejunum, ileum and colon. Collectively, both the intestinal environment and the adhesion ability of *L. plantarum* AR113 affected intestinal colonization, and the host's intestinal genetic background may be a key factor in the intestinal colonization of *L. plantarum*.

1. Introduction

Lactobacillus plantarum (recently reclassified as *Lactiplantibacillus (L.) plantarum* (Zheng et al., 2020)) is widely distributed in nature and present in the gastrointestinal tract of humans and animals (Seddik et al., 2017). *L.plantarum*, one of the important probiotic, has been shown to be involved in a variety of probiotic functions (e.g., the alleviation of enteritis (Jang et al., 2014; Satish Kumar et al., 2015), improvement of lactose intolerance and lowering cholesterol (Wang et al., 2009), and the sustainability of these probiotic function is predicated on their ability to colonization the host intestinal (Buntin et al., 2017). However, as the host gastrointestinal tract is composed of a myriad of dynamic and diverse environments created by microbial metabolism and the host's attempts to regulate physical and chemical parameters (e.g. temperature, pH, water), it is not easy for probiotics to colonize the intestine.

The intestinal epithelium mucus layer consists mainly of complex glycoproteins (mucins), which protect the host epithelial cells from damage and also provide habitat and nutrition for the intestinal flora. Therefore, the adhesion of bacteria to the mucin layers provides sufficient time for these bacteria to remain in the intestine, preventing their rapid elimination from the body through peristalsis of the gastrointestinal tract. Bacterial adhesion also plays an important role in the large-scale establishment and colonization of strains on host target sites (Muñoz-Provencio et al., 2009). Bacterial adhesion can be divided into non-specific and specific adhesion depending on the mechanism of action. Non-specific adhesion occurs during hydrophobic and electrostatic interactions, affecting the attractive and repulsive forces between the cell and the mucosal surface, and thus regulating the adhesion level (Hamadi et al., 2012). Meanwhile, specific adhesion occurs through

* Corresponding author at: University of Shanghai for Science and Technology, 516 Jungong Road, Shanghai 200093, China.
E-mail address: 1015wanggq@163.com (G. Wang).

https://doi.org/10.1016/j.foodres.2022.111382
Received 23 March 2022; Received in revised form 8 May 2022; Accepted 13 May 2022
Available online 17 May 2022

specific adhesion-receptor binding and is an important mechanism for bacterial adhesion colonization of the host gastrointestinal surface. Certain proteins such as mannose-specific mucin, s-layer proteins, glyceraldehyde-3-phosphate dehydrogenase, elongation factor-Tu and mucus-binding proteins play important roles in bacterial adhesion to mucus proteins (Buntin et al., 2017). To assess the effect of these surface proteins on bacterial adhesion, they are often treated with protein denaturing agents (e.g., lithium chloride, guanidine hydrochloride, or proteinase K), or protein extracts are added to bacteria and verified by cell adhesion assays, which in turn predict whether the protein mediates bacterial adhesion to the host intestinal mucus layer (Carasi et al., 2014).

In addition, the establishment and colonization of probiotics has been shown to vary significantly according to the hosts' genetic backgrounds (Ganesh et al., 2018; Marco et al.,2007;Marco et al.,2009; Zhou et al.,2019). Disturbance of the host's original intestinal microbial community might facilitate the colonization of probiotic bacteria, similar to "priority effects", which is achieved by the preemption or modification of ecological niches (Litvak et al., 2019). The use of antibiotics including amoxicillin (beta-lactam), ciprofloxacin (fluoroquinolone) and doxycycline (tetracycline) have been reported to achieve reductions in the relative abundances of intestinal flora (Cabral et al., 2019). Meanwhile, administration of the laxative polyethylene glycol (PEG) to mice triggered mild osmotic diarrhea and altered the alpha and beta diversity of the intestinal microbes, but without causing intestinal histological inflammation and destruction to the host epithelial cells (Tropini et al., 2018). Importantly, intestinal strain tracer methods play an important role in the assessment of their intestinal colonization. Red fluorescent protein (RFP), which was first reported on 1999, has a longer excitation and emission wavelengths and covers wavelengths not covered by green fluorescent protein (GFP). RFP results in better tissue penetration imaging and weaker background light intensity, and is widely used in biological studies (Matz et al., 1999).

In this work, we aimed to investigate the influence of *L. plantarum*'s adhesion ability and the host environment on its intestinal colonization. Seven mucin genes in the *L. plantarum* AR113 genome were knocked out and the RFP gene was tagged using our group's well established CRISPR-Cas9 gene editing technology. Wild-type and knockout strains were evaluated for acid and bile salt tolerance, surface properties (hydrophobicity, auto-aggregation and co-aggregation) and adhesion to HT-29 cells. Importantly, we further investigated the ability of AR113 to colonization in vivo, and CFDA-SE labeling was used to detect dissemination and distribution in the intestine.

2. Materials and methods

2.1. Bacterial strains, cells, animals and culture conditions

L. plantarum AR113 was previously isolated from traditional Chinese kimchi, identified and sequenced by Shanghai Miki Biological Co., Ltd (Lin et al., 2020). The strains and plasmids used in this study are listed in supplement Table 1. *E. coli* Top 10 was used as a host for molecular cloning, and was grown at 30℃ in Luria-Bertani broth (LB). The wild-type strain and knockout strains were cultured statically at 37℃ in deMan Rogosa and Sharpe (MRS) medium. Antibiotics were supplemented at the following concentrations when needed: 50 μg/mL kanamycin for *E. coli* Top 10, and 10 μg/mL each of erythromycin and chloramphenicol for *L. plantarum*.

The human adenocarcinoma cell line HT-29 was purchased from the Cell Resources Center of Shanghai Institutes for Biological Sciences (Shanghai, China). HT-29 cells were cultivated in 1640 medium (Gibco™, Thermo Fisher Scientific, Grand Island, USA) containing 10% fetal bovine serum at 37 °C under 5% CO_2. The number of replicates was three for all experiments performed.

Male C57 BL/6 mice (Purchase from jiesijie, Shanghai, China) . The mice were housed in an air-conditioned room with the laboratory temperature maintained at 23 ± 2℃ and a relative humidity of 50 ± 10%. All mice were housed for acclimatization for at least one week before the following experiments, and the procedures were performed according to institutional and governmental regulations about the use of experimental animals. All animal procedures were performed in accordance with the Guidelines for Care and Use of Laboratory Animals of Shanghai Jiao Tong University and approved by the Animal Ethics Committee of Shanghai Jiao Tong University.

2.2. Plasmid construction

The primers needed to construct the gene knockout plasmid of *L. plantarum* AR113 are shown in supplement Table 2. Taking *Lp*_0819 as an example, the skeleton of pHSP01 was obtained by double digestion with *Apa*I (Cat.1604, Takara, Japan) and *Xba*I enzymes (Cat.1643, Takara, Japan), and two 1.5 kb fragments flanking *Lp*_0819 (0819-up and 0819-down) were amplified from *L. plantarum* AR113 by polymerase chain reaction (PCR) using 0819-up-F/0819-up-R and 0819-down-F/0819-down-R. A 103 bp guide RNA (single guide [sg]-RNA) was amplified from pHSP01 by PCR using sgRNA-F/sgRNA-R. The up, down, and sgRNA fragments were fused by overlapping extension PCR using 0819-up-F/0819-sgRNA-R to generate a *Lp*_0819-up-down-sgRNA fragment. Then, the fragment *Lp*_0819-up-down-sgRNA was assembled into the plasmid backbone (pHSP01 linearized by enzymes *Apa*I and *Xba*I) using a single-step cloning kit (Cat.C112-01, Vazyme, China).

2.3. Construction of knockout strains

In this study, the cluster regularly interspaced short palindromic repeat (CRISPR)-CRISPR-associated protein 9 (Cas9) system was used to construct the mucin knockout strain, and the process is shown in Fig. 1. First, the upstream and downstream homologous arms of the gene at the knockout or insertion site are ligated to the sgRNA (up-down-sgRNA), and up-down-sgRNA fragments are cloned with the editing plasmid *pLH01* skeleton (digested by ApaI and XbaI) by one-step cloning to obtain the knockout or insertion plasmid. Next, the Helper Plasmid pHSP01 was introduced into *L. plantarum* AR113 by electrotransformation to obtain AR113(pHSP01). Finally, the knockout or insertion plasmid was then introduced into *L. plantarum* AR113 (*pHSP01*) in the same manner, screened in erythromycin and chloramphenicol resistance plates, and the target strain was obtained after verification by sequencing. The preparation of electrocompetent cells and the electro-transformation of *L. plantarum* WCFS1 was performed as previously described, with certain modifications (Huang et al., 2019). In brief, a 3% (v/v) inoculum of the overnight culture was transferred into 50 mL of fresh SGMRS medium (MRS with 1% glycine) supplemented with an antibiotic when needed. The cells were recovered by centrifugation at 2105*g* and 4℃ when the optical density at 600 nm (OD) (DU-800, Beckman Coulter, USA) reached 0.3–0.5. The cell pellet was washed twice with 1 mM of $MgCl_2$ and resuspended in 0.5 mL of SM buffer (952 mM of sucrose and 3.5 mM of $MgCl_2$). Competent cells were aliquoted and stored at − 80℃. Electroporation was performed with a Gene Pulser Xcell System (MicroPulser, Bio-Rad, USA) in a 2 mm cuvette (165–2086, Bio-Rad, USA) with the following parameters: 2.5 kV, 200 Ω, and 25 μF. Then, 1 mL of the recovery medium (MRS with 500 mM of sucrose, 20 mM of $MgCl_2$, and 2 mM of $CaCl_2$) was added into a cuvette, and the mixture was incubated for 2 to 3 h and plated on MRS agar supplemented with an antibiotic. Construction of RFP gene recombinant bacteria is consistent with the above.

2.4. Acid and bile salt tolerance test

Bacterial tolerance to acid and bile salts was assessed as described by Mishra and Prasad, with appropriate modifications (Matz et al., 1999). Acid tolerance was assessed by adjusting the MRS liquid medium pH with 10 M of HCl to 3.0, 3.5 and 4.0, and bile salt tolerance was assessed

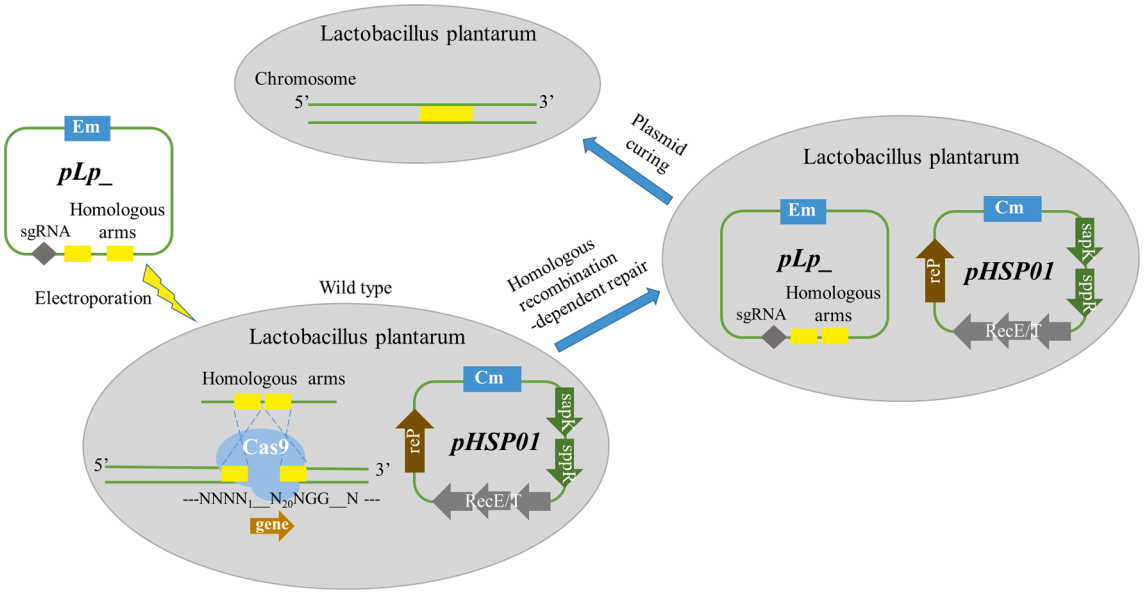

Fig. 1. The process of constructing knockout strain.

by adding 0.2% w/v, 0.3% w/v and 0.4% w/v of bile salt to the MRS liquid medium and sterilizing it. Wild-type and knockout strains were incubated overnight and the OD_{600} values of the bacterial suspensions were adjusted to the same level and 3% v/v inoculum was inoculated into the acid and bile salt-adjusted MRS liquid mediums. After mixing, 200 μL of the medium was placed on a sterile plate, and the uninoculated MRS liquid medium was used as the reference. The culture solution was incubated at 37℃ for 24 h and the OD_{600} was measured every 30 min and recorded by fully automated growth curve analyzer (Bioscreen C, oy growth curves ab ltd, Finland). Three replicates were made for each sample.

2.5. Auto-aggregation and co-aggregation assays

Auto-aggregation assays were performed according to Collado (Collado et al., 2007), with certain modifications. Bacteria were grown for 18 h at 37℃ in MRS liquid medium. The bacteria were harvested by centrifugation at 5000*g* for 15 min, washed twice and resuspended in phosphate buffered saline (PBS) at pH 7.2. OD_{600} was adjusted to 0.25 ± 0.05 to obtain viable bacteria counts of approximately 10^8 colony forming units (CFU)/mL. Cell suspensions (5 mL) were mixed by vortex for 15 s and auto-aggregation was determined at different incubation times (0 and 5 h) at room temperature without agitation. The auto-aggregation percentage was expressed as:

$$R_{AA} = \frac{A_0 - A_t}{A_t} \times 100\%$$

where A_t represents the absorbance at time t = 5 h and A_0 represents the absorbance at t = 0 h.

The method for preparing the bacterial suspensions for co-aggregation was the same as that for the auto-aggregation assay. Equal volumes (2 mL) of cell suspension were mixed together in pairs by vortexing for 15 s. Control tubes were set up at the same time. The OD_{600} of the suspensions was measured at different incubation times (0 and 5 h) at room temperature without agitation. The percentage of co-aggregation was calculated using the equation:

$$R_{CA} = \frac{A0 + A1 - 2Amix}{A0 + A1} \times 100\%$$

where A_0 and A_1 represent the OD_{600} of the two strains in the control tubes, and A_t represents the OD_{600} of the mixed bacterial suspensions at 5 h.

2.6. Measurement of bacterial hydrophobicity

Bacterial suspensions were prepared as described above. OD_{600} was adjusted to 0.25 ± 0.05, then an equal volume of xylene (Sinopharm Chemical Reagent Co., Ltd, Shanghai, China) was added. The two-phase system was thoroughly mixed by vortex for 3 min. The OD_{600} of the aqueous layer was measured and the hydrophobicity percentage was expressed as.

$$R_{HC} = \frac{A0 - At}{At} \times 100\%$$

where A_t represents the absorbance at time t = 1 h and A_0 represents the absorbance at t = 0 h.

2.7. L. plantarum adhesion to HT-29 cells

Cell adhesion experiments were performed as previously described (Wang et al., 2019), with some modifications. Bacteria were harvested by centrifugation (3145*g*, 10 min) and washed twice with PBS (pH 7.2), then resuspended in Roswell Park Memorial Institute (RPMI) 1640 culture medium. The bacterial suspension concentration was adjusted to 10^8 CFU mL^{-1}. Cells from a colon cancer cell line (HT-29) were cultured in 12-well plates. When the cells covered 80–90% of the plates, they were rinsed twice with PBS, and 1 mL of *L. plantarum* suspension (10^8 CFU mL^{-1}) and 1 mL of 1640 culture medium were added to each well. The plates were placed in a cell incubator at 37 ℃ for 2 h in a 5% CO_2 atmosphere. After incubation, each well in the plates was washed three times with PBS (pH 7.2) to remove free, non-attached bacteria cells, followed by methanol fixation (1 mL) for 20 min, PBS rinsing twice, gram staining, and microscopic observation. Twenty views were randomly chosen for imaging. The adhesion number of *L. plantarum* to HT-29 cells was calculated on the basis of 100 cells. The experiment was repeated in triplicate.

2.8. Flow cytometry analysis

Fluorescent labeling of the strains was performed as described in previous studies (Lee et al., 2004). The concentration of the L. plantarum

suspension was adjusted with PBS to 10^9 CFU mL^{-1}. The bacterial suspension was mixed with 5-(6)-carboxyfluorescein diacetate N-succinimidyl ester (cFDA-SE) (50 μM, in ethanol) in equal volumes, followed by incubation in a 37 °C water bath for 20 min in the dark. The cell mass was collected by centrifugation at 8000*g* for 3 min and rinsed with PBS twice to remove unreacted cFDA-SE. Flow cytometry (FACSCalibur, BD Bioscience, USA) was used to detect the cell fluorescent labeling percentage. The experiment was repeated in triplicate.

2.9. Animal experiments

In vivo colonization experiments were performed according to previous research (Lee et al., 2004) with some modifications. Animals were grouped for in vivo colonization experiments as shown in Fig. 5 A. Six-week-old male C57 BL/6 mice were allowed to drink and eat freely, and were divided into control and experimental groups, with four mice in each group. In the experimental groups, each mouse was gavaged with the bacterial solution (the fluorescence intensity of the bacterial solution was adjusted to 2×10^4) for 6 days, and the control group was gavaged with an equal volume of sterile water. In vivo reproduction experiments. Six-week-old male C57 BL/6 mice were allowed to drink and eat freely, and 12 mice were each allocated to the control and experimental (AR113-RFP and AR113Δ*Lp*_1431Δ*Lp*_2233Δ*Lp*_2792-RFP) groups. Each mouse in the experimental groups was gavaged with 5×10^9 CFU of the strains for 1 day, and the normal control group was gavaged with an equal volume of sterile water.

The intestinal flora abundance treatment was performed according to the previous research (Tropini et al., 2018). The experimental grouping protocol was referred to Fig. 4A, and the only difference was that 15% w/v PEG was added to the drinking water of the mice. In the experimental group, each mouse was gavaged with bacterial solution (the fluorescence intensity of the bacterial solution was adjusted to 2×10^4) for 6 days, and the control group was gavaged with an equal volume of sterile water.

2.10. Fecal collection and treatment

Feces were collected before, during and after the mice were gavaged with the bacterial strains, as described in previous studies (Fornelos et al., 2020). The sterile tubes (1.5 mL) used were sterilized and the forceps used for collection were disinfected before collection. During fecal collection, each mouse was placed in a cage sterilized with alcohol and on a clean sheet of paper, and the feces was collected after the mouse had defecated. The forceps were disinfected after each use.

Fecal handling was performed as described in previous research (Tuo et al., 2013), with some modifications. 0.025 ± 0.005 g of feces per mice was collected and placed into round-bottomed sterile tubes (2 mL) with a 5 mm diameter steel strain. Then, 1 mL of sterilized PBS buffer was added to each sterile tube, followed by homogenization using a homogenizer at 1000 rpm for 3 min. The solution was then centrifuged at 400 × g at 4 °C for 3 min, and the supernatant was collected and filtered using a 300-mesh filter, 200 μL of each well was placed in a black flat-bottomed 96-well plate, the fluorescence intensity was measured at the excitation wavelength of 600 nm and the emission wavelength of 635 nm using an enzyme marker (SpectraMax i3x, Molecular Devices, USA). Feces of mice not administered with bacteria were used as control, the experiment was repeated in triplicate.

2.11. Intestinal tissue collection

The mice were euthanized by decapitation, and the duodenum, jejunum, ileum and colon were collected at a length of 2 cm. The intestinal contents were collected, then the intestine was dissected longitudinally along the intestine and the mucosal layer was scraped with a coverslip into a 2 mL sterility tube, to which 1 mL of sterilized PBS buffer was added. The rest of the procedure followed the fluorescence intensity assay or the flow cytometry method. The experiment was repeated in triplicate.

2.12. Statistical analysis

Significant differences among the data were examined using one-way ANOVA and Duncan's test with Statistical Product and Service Solutions (V17.0, SPSS, USA) software. The significance of the correlation coefficient was also examined. Data are presented as means with standard deviations and significant differences ($p < 0.01$) are presented with different letters. Data measured by the fully automated growth curve analyzer were simulated using the Gompertz growth level model to obtain maximum biomass, hysteresis time and maximum specific growth rate. GraphPad Prism software (8.0.1.244, GraphPad Software, USA) was used for to plot the graphs.

3. Results

3.1. Construction and physiological characterization of knockout strains

The successfully sequenced knockout plasmids and knockout strains are shown in Fig. 2 A–G. The knockout strains were named as AR113△*Lp*_0819, AR113△*Lp*_1080, AR113△*Lp*_1431, AR113△*Lp*_2233, AR113△*Lp*_2739, AR113△*Lp*_2792, AR113△*Lp*_2805, AR113△*Lp*_1431 △*Lp*_2792, and AR113△*Lp*_1431△*Lp*_2233△*Lp*_2792. Next, we measured the physiological characteristics of the mentioned wild-type and knockout strains. We found that the growth trend of all strains was consistent in liquid MRS (Fig. 3 A, Table 1). In addition, we also measured the hydrophobicity, auto-aggregation, and co-aggregation ability of *L. plantrum*, as well as its ability to adhere to HT-29 are shown in Fig. 3 B, due to the fact that these surface physiological properties of probiotics are among the most important indicators to assess their ability to colonize in vivo. The hydrophobicity of the strains ranged from 80.62% to 98%, all of which showed strong hydrophobicity. The wild-type strain had the lowest hydrophobicity (80.62%) and AR113Δ*Lp*_1431△*Lp*_2792△*Lp*_2233 had the highest hydrophobicity (98.00%), with significant differences between both knockout strains and wild-type strain. The auto-aggregation ability of the strains varied greatly. AR113△*Lp*_1431 had the least auto-aggregation ability (11. 29%) and AR113△*Lp*_2805 had the greatest auto-aggregation ability (32.14%). In terms of co-aggregation ability, AR113Δ *Lp*_1431 had the least co-aggregation ability (11.22%), which was significantly different from the wild-type strain, and AR113△*Lp*_2233 had the greatest co-aggregation ability (26.59%).

The adhesion is an important indicator to assess the ability of probiotic bacteria to colonization in vivo. In the adhesion assay with HT-29 cells (Fig. 3 B), some single knockout strains showed an increase in the adhesion number, for example, AR113Δ*Lp*_1080 had 196 ± 6 CFU per 100 cells and AR113Δ*Lp*_2792 had 199 ± 9 CFU per 100 cells; some single knockout strains showed a decrease in the adhesion number, for example, AR113Δ*Lp*_1431 had 159 ± 17 CFU per 100 cells and AR113Δ*Lp*_2233 had 171 ± 9 CFU per 100 cells. However, these single knockout strains were not significantly different from AR113, which had 175 ± 25 CFU of adhesion per 100 cells. Based on these results it cannot be proven which genes are more important than others. We propose that the possible reason is the existence of genetic complementation and also analyzed the domain organization of these mucins. Compared to other mucin genes, the highest number of repeated MucBP domains (pfam06458) was found in *Lp*_1431 and *Lp*_2792, MucBP domain and LPXTG anchoring motif (pfam00746) were present in *Lp*_2233. Therefore, we performed a combinatorial knockout. Among the combined knockout strains, AR113Δ*Lp*_1431Δ*Lp*_2792Δ *Lp*_2233 had an adhesion number of 114 ± 8 CFU per 100 cells, which was significantly different from AR113.

To assess the acid tolerance of the strains, the initial pH of the MRS broth medium was adjusted to 3.0, 3.5 and 4.0 to examine the growth of the strains at different pH levels (Fig. 3 C-E). The measured growth

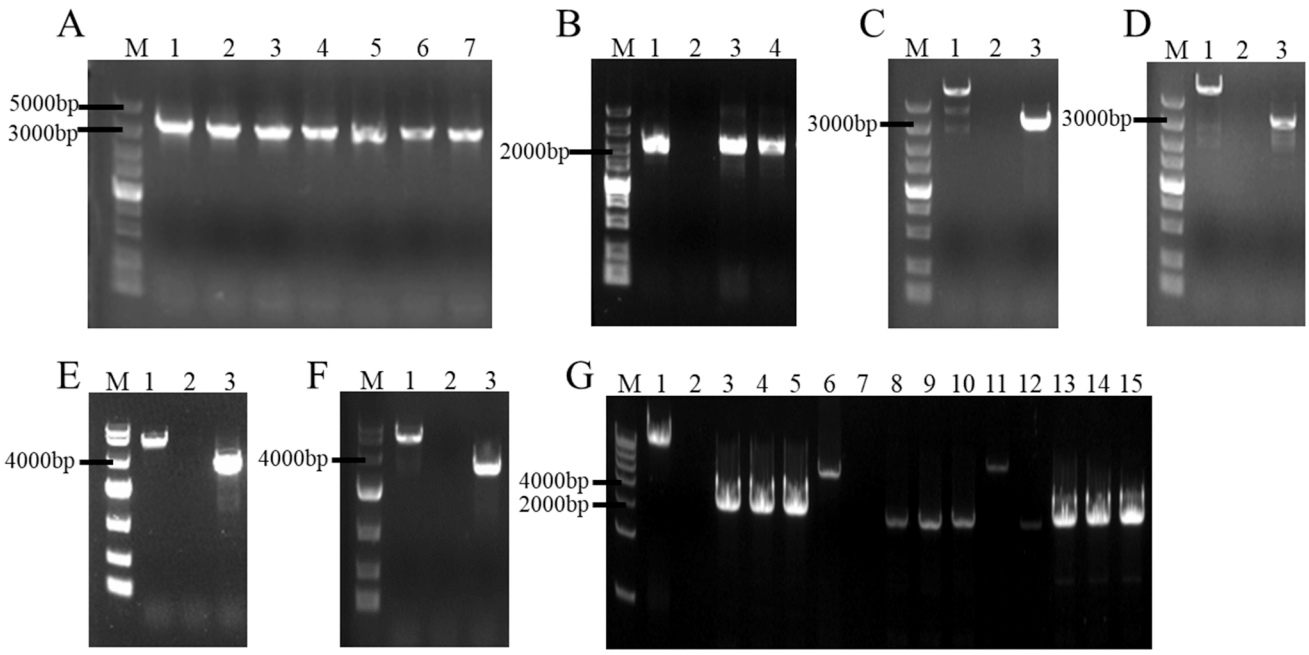

Fig. 2. Construction of knockout strains. A: M:5000bp Marker, Line1:p*Lp*-0819;Line2:p*Lp*_1080; Line3: p*Lp*_1431;Line4:p*Lp*_2233; Line5:p*Lp*_2739; Line6:p*Lp*_2792. B: M:5000bp Marker, Line1:pHSP01, Line2: negative control,Line3:AR113(pLH01). C: M:5000bp Marker, Line1:AR113,Line2: negative control, Line3: AR113Δ*Lp*_2805. D: M:5000bp Marker, Line1:AR113, Line2:negative control, Line3: AR113Δ*Lp*_0819. E:M:10000bp Marker, Line1:AR113, Line2:negative control, Line3: AR113Δ*Lp*_1080. F:M:10000bp Marker,Line1: AR113,Line2: negative control, Line3: AR113Δ*Lp*_2739. G:M:10000bp Marker, Line1,6,11: AR113, Line 2,7,12: negative control, Line 3,4:AR113△*Lp*_1431,Line5,10,15:AR113△*Lp*_1431 &2233&2792, Line8,9:AR113△*Lp*_ 2233, Line 13,14:AR113△*Lp*_2792.

curves were also fitted to obtain the maximum biomass, hysteresis time and maximum specific growth rate of the wild-type and knockout strains (Table 2). Overall, the growth of the knockout and wild-type strains showed a consistent growth trend. It is noteworthy that none of the strains grew at pH 3.0, as the pH increased, the maximum biomass and maximum specific growth rate of the strains increased and the lag time decreased.

The bile salt concentration in the MRS medium was adjusted to 0.2 % w/v, 0.3% w/v and 0.4% w/v, and the strains were incubated in the medium for 24 h at 37 °C to assess the tolerance of the strains to bile salts (Fig. 3 F-H). The maximum biomass, hysteresis time and maximum specific growth rate were obtained by fitting the curves (Table 3). At a bile salt concentration of 0.2 %w/v, compared with the wild-type strain, AR113Δ*Lp*_0819, AR113Δ*Lp*_1080 and AR113Δ*Lp*_2805 showed an increase in maximum biomass of 0.27–0.3, and the other knockout strains were not significantly different from the wild-type strain. While the bile salt concentration was increased to 0.4% w/v, some mutant strains (AR113Δ*Lp*_1431, AR113Δ*Lp*_2233, AR113Δ*Lp*_2792, AR113Δ*Lp*_1431Δ*Lp*_2792, AR113Δ*Lp*_1431Δ*Lp*_2233Δ*Lp*_2792) showed a significant increase in bile salt tolerance compared to wild-type strains, with an increase in maximum biomass of 0.18–0.25 and a decrease in lag time of 2.69–3.17 h. However, some mutant strains (AR113Δ*Lp*_1080, AR113Δ*Lp*_2739, AR113Δ*Lp*_2805) were not tolerated at this bile salt concentration and showed growth stagnation (the maximum biomass was near zero). These results suggest that different mucin genes differ for the growth of the strains in different bile salt concentrations. The maximum biomass and maximum specific growth rate of all strains were lower and the hysteresis time increased at higher bile salt concentrations compared to bile salt-free conditions. In other words, *Lp*_1431, *Lp*_2233, *Lp*_2792 may affect bile salt tolerance in *L.plantarum*.

Based on Pearson correlation analysis (Fig. 3 I-K), the bacteria auto-aggregation and co-aggregation did not correlate with adhesive ability ($r = -0.02$, $r = 0.16$, respectively). While there was a negative correlation between the hydrophobicity and adhesive ability of *L. plantarum* ($r = -0.30$).

3.2. Red fluorescent protein gene insertion

We will select AR113 and AR113Δ*Lp*_1431Δ*Lp*_2233Δ*Lp*_2792 for further in vivo experiments based on the results of in vitro adhesion experiments. We inserted the red fluorescent protein (RFP) gene into the *L. plantarum* genome, and the fluorescence intensity of the bacteria was measured in mouse feces and intestine to assess the ability of the *L. plantarum* to colonize the intestinal. The RFP gene was inserted into the AR113 and AR113Δ*Lp*_1431Δ*Lp*_2233Δ*Lp*_2792 genome and the bacterial solution concentrations of the AR113, AR113-RFP, AR113Δ*Lp*_1431Δ*Lp*_2233Δ*Lp*_2792 and AR113Δ*Lp*_1431Δ*Lp*_2233Δ *Lp*_2792-RFP were adjusted to the same OD_{600} values. The results showed that the fluorescence intensity of AR113-RFP, AR113Δ*Lp*_1431Δ*Lp*_2233Δ*Lp*_2792-RFP was significantly higher than that of AR113, AR113Δ*Lp*_1431Δ*Lp*_2233Δ*Lp*_2792, respectively ($p < 0.01$). In addition, when AR113-RFP and AR113Δ*Lp*_1431Δ*Lp*_2233Δ*Lp*_2792-RFP were mixed with other bacteria or substances, the fluorescence intensity was much higher than that of the control, which also provides a theoretical basis for the in vivo detection of the strains (Fig. 4 C-D).

3.3. Determination of in vivo colonization ability

In vitro experiments are unable to simulate the complex in vivo environment, and thus it was necessary to explore in vivo colonization of the strain. The stain AR113Δ*Lp*_1431Δ*Lp*_2233Δ*Lp*_2792-RFP was selected for the in vivo experiments, as it was a strain that was significantly different from AR113 in the in vitro cell adhesion assay. AR113-RFP reached its highest fluorescence intensity of 6.031×10^4 one day after the end of gavage, and AR113Δ*Lp*_1431Δ*Lp*_2233Δ*Lp*_2792-RFP had the highest fluorescence intensity of 3.824×10^4 on the second day after gavage. Thereafter, AR113-RFP showed a gradual decrease with time, reaching its lowest fluorescence intensity of 0.59×10^4, however, AR113Δ*Lp*_1431Δ*Lp*_2233Δ*Lp*_2792-RFP showed a wavelike decrease and fluorescence was not detected in the feces at 14 days (Fig. 5 B).

When the fluorescence intensity of different loci in the mouse intestine was examined (Fig. 5 C), AR113-RFP did not demonstrate fluorescence in

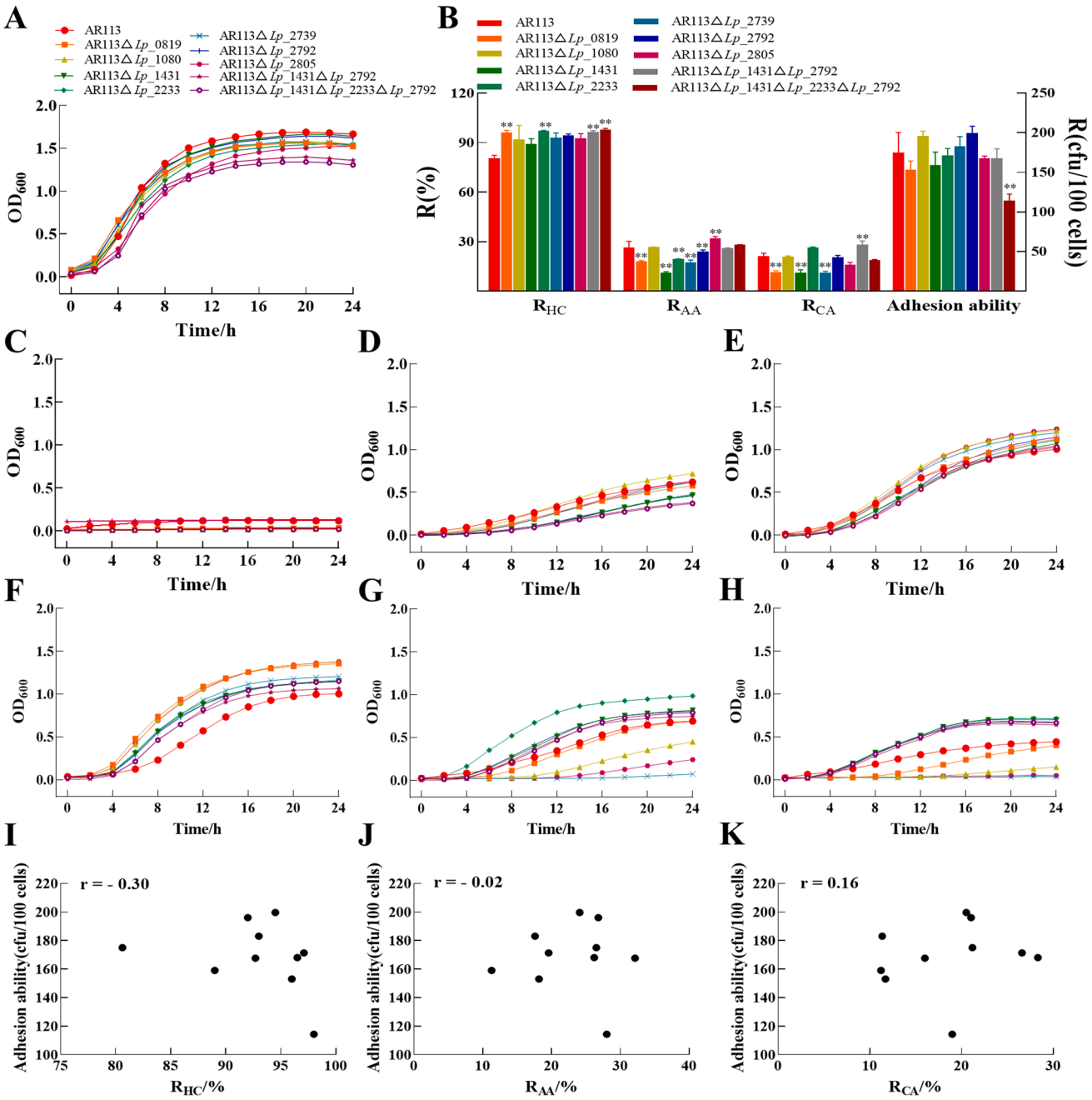

Fig. 3. Measurement of the growth and physiological characteristics of the strains. A: growth curves of wild-type and adherent knockout strains in MRS. B: Hydrophobicity, auto-aggregation, co-aggregation ability and adhesion ability of the strains. C-E: growth of the strains in MRS broth at pH 3.0, 3.5, and 4.0, respectively. F-H: Growth of the strains in MRS broth with bile salt concentrations of 0.2% w/v, 0.3% w/v and 0.4% w/v, respectively. I-K: The correlation between R_{HC}, R_{AA}, R_{CA} and adhesion ability of the strains (AR113, AR113Δ*Lp*_0819, AR113Δ*Lp*_1080, AR113△*Lp*_1431, AR113△*Lp*_ 2233, AR113Δ*Lp*_2739, AR113△*Lp*_2792, AR113△*Lp*_2805, AR113△*Lp*_1431△*Lp*_2792, AR113△*Lp*_1431△*Lp*_2233△*Lp*_2792). Data are represented as means ± standard deviations, each experiment was repeated in triplicate (n = 3). **Means differ significantly ($P < 0.01$). The Pearson correlation coefficient (r), r values between −1 and + 1, where 1 indicates a positive linear correlation and −1 is a negative linear correlation.

both the duodenum and jejunum. Fluorescence was detected in both the ileum and colon with fluorescence intensities of 0.120×10^4 and 0.105×10^4, respectively, and AR113Δ*Lp*_1431Δ*Lp*_2233Δ*Lp*_2792-RFP was not detected in the duodenum, jejunum, ileum and colon.

The wild-type and knockout strains were labeled with the fluorescent dye cFDA-SE to investigate the distribution of *L. plantarum* in the gut, and the labeling rate was detected by flow cytometry. The results are shown in Fig. 5 D-E. The fluorescent dye labeling rate of all strains was greater than 98%, enabling further animal experiments to be performed. Mice were gavaged with the cFDA-SE labeled strains and the adhesion of the fluorescently labeled strains in the intestine was detected by flow cytometry at 3 h, 24 h, 48 h and 72 h after gavage.

The colonization numbers of AR113-RFP and AR113Δ*Lp*_1431Δ*Lp*_2233Δ*Lp*_2792-RFP in the duodenum and its intestinal lumen gradually decreased, while the colonization numbers in the jejunum, ileum and colon and its intestinal lumen showed an increase after 24 h of gavage. Notably, after the end of gavage, AR113 had the highest colonization number in the duodenum (53 ± 9 CFU) and in the long intestinal lumen of the colon (5952 ± 460 CFU) AR113Δ*Lp*_1431Δ*Lp*_2233 Δ*Lp*_2792-RFP had the highest colonization numbers in the colonic mucosa

Table 1
Maximum biomass, retardation time and maximum specific growth rate of strains in MRS.

Strains	Maximum biomass (OD_{600})	Hysteresis time (h)	Maximum specific growth rate (OD_{600}/h)
AR113	1.67	2.33	0.33
AR113△*Lp*_0819	1.55	2.89	0.27
AR113△*Lp*_1080	1.57	2.94	0.27
AR113△*Lp*_1431	1.65	2.72	0.30
AR113△*Lp*_2233	1.55	3.08	0.29
AR113△*Lp*_2739	1.57	2.92	0.23
AR113△*Lp*_2792	1.62	2.74	0.24
AR113△*Lp*_2805	1.53	3.41	0.22
AR113Δ*Lp*_1431&2792	1.37	2.27	0.31
AR113Δ*Lp*_1431Δ*Lp*_2233Δ*Lp*_2792	1.32	2.31	0.25

and intestinal lumen, at 870 ± 293 CFU and 76 ± 17 CFU, respectively. At 48 h, the wild-type strain had the highest colonization numbers in the colonic mucosa and intestinal lumen at 56 ± 15 CFU and 1925 ± 158 CFU, respectively, while the knockout strain had the highest colonization numbers in the ileal mucosa and intestinal lumen at 28 ± 5 CFU and 51 ± 3 CFU, respectively. Subsequently, the colonization numbers in the mucosa and intestinal lumen decreased for both strains. Remarkably, both AR1113-RFP and AR113Δ*Lp*_1431Δ*Lp*_2233Δ*Lp*_2792-RFP colonized mainly in the colon (Fig. 5 F-G).

In addition, *L. plantarum* showed a wave-like change in the colonization numbers of both the mucosal layer and the intestinal lumen of mice, and the colonization number of AR113-RFP was higher than that of AR113Δ*Lp*_1431Δ*Lp*_2233Δ*Lp*_2792-RFP (Fig. 5 H). The colonization numbers of both strains showed an increase between 24 and 48 h of gavage, from 264 ± 43 CFU to 2224 ± 223 CFU for AR113-RFP and from 186 ± 57 CFU to 221 ± 49 CFU for AR113Δ *Lp*_1431Δ*Lp*_2233Δ*Lp*_2792-RFP, where the difference between the two strains in the intestinal mucosal layer was smaller at 48 h, but in the intestinal lumen, the number of wild-type strains was approximately 10 times higher than that of the knockout strain (Fig. 5 H).

3.4. Colonization ability of L. plantarum in the PEG-treated intestine

The effect of the intestinal environment on the gut colonization of the strains was investigated further. Mice with 15% PEG in their drinking water showed significant weight loss and watery feces (Fig. 6 A, C), but no blood in the stool. The fluorescence intensity of AR113-RFP was found to reach a maximum of 3.529×10^4 on the fourth day of gavage, and AR113Δ *Lp*_1431Δ *Lp*_2233Δ *Lp*_2792-RFP reached a maximum on the sixth day of gavage. Both showed a tendency to rebound on the second day after the end of gavage, which was consistent with the results of control group, but thereafter the fluorescence intensity of both gradually decreased with time. Fluorescence was not detected in the duodenum for both AR113-RFP and AR113Δ*Lp*_1431Δ*Lp*_2233Δ*Lp*_2792-RFP, while fluorescence was detected in the jejunum, ileum and colon. The highest fluorescence intensity of 1.063×10^4 for AR113-RFP was detected in the ileum and the lowest fluorescence intensity of 0.368×10^4 was detected in the colon. AR113Δ*Lp*_1431Δ*Lp*_2233Δ*Lp*_2792-RFP had the highest fluorescence intensity of 0.570×10^4 in the jejunum and the lowest 0.089×10^4 (Fig. 6 B, D).

4. Discussion

The adhesion to the host mucosal surface is essential for the colonization of probiotics in the host intestine. Adhesion is mainly achieved by binding of mucins (mucins, lipoteichoic acid, polysaccharides, etc.) on the surface of probiotic bacteria to specific receptors on the host intestinal epithelium. Numerous studies on the function of mucins (lp_0964, lp_1229, lp_1643, lp_2486, lp_3059, lp_3114, lp_3127) of *L. plantarum* have been carried out mainly through in vitro cell adhesion

Table 2
Maximum biomass, retardation time and maximum specific growth rate of strains in MRS at different pH levels.

Strains	Maximum biomass (OD_{600})				Hysteresis time (h)				Maximum specific growth rate (OD_{600}/h)			
	Control	pH3.0	pH3.5	pH4.0	Control	pH3.0	pH3.5	pH4.0	Control	pH3.0	pH3.5	pH4.0
AR113	1.67	–	0.76	1.04	2.33	–	8.35	5.13	0.33	–	0.05	0.11
AR113Δ*Lp*_0819	1.55	–	0.71	1.17	2.89	–	7.84	5.31	0.27	–	0.05	0.09
AR113Δ*Lp*_1080	1.57	–	0.85	1.27	2.94	–	7.07	4.86	0.27	–	0.05	0.10
AR113Δ*Lp*_1431	1.65	–	0.71	1.17	2.72	–	9.02	5.92	0.30	–	0.03	0.08
AR113Δ*Lp*_2233	1.55	–	0.73	1.21	3.08	–	9.11	5.76	0.29	–	0.03	0.08
AR113Δ*Lp*_2739	1.57	–	0.79	1.24	2.92	–	7.87	4.80	0.23	–	0.04	0.10
AR113Δ*Lp*_2792	1.62	–	0.63	1.23	2.74	–	7.99	5.12	0.24	–	0.03	0.09
AR113Δ*Lp*_2805	1.53	–	0.80	1.30	3.41	–	7.51	4.97	0.22	–	0.04	0.10
AR113Δ*Lp*_1431&2792	1.37	–	0.53	1.11	2.27	–	8.21	5.03	0.31	–	0.02	0.08
AR113Δ*Lp*_1431Δ*Lp*_2233Δ*Lp*_2792	1.32	–	0.47	1.09	2.31	–	7.35	4.84	0.25	–	0.03	0.09

Table 3
Maximum biomass, retardation time and maximum specific growth rate of strains in MRS with different bile salt concentrations.

Strains	Maximum biomass (OD_{600})				Hysteresis time (h)				Maximum specific growth rate (OD_{600}/h)			
	Control	0.20%	0.30%	0.40%	Control	0.20%	0.30%	0.40%	Control	0.20%	0.30%	0.40%
AR113	1.67	1.08	0.88	0.50	2.33	4.68	7.80	7.01	0.33	0.10	0.07	0.04
AR113Δ*Lp*_0819	1.55	1.35	0.79	0.58	2.89	3.65	5.73	8.21	0.27	0.17	0.07	0.04
AR113Δ*Lp*_1080	1.57	1.38	0.78	–	2.94	3.70	9.11	–	0.27	0.16	–	–
AR113Δ*Lp*_1431	1.65	1.15	0.85	0.74	2.72	3.65	4.54	4.16	0.30	0.13	0.07	0.07
AR113Δ*Lp*_2233	1.55	1.15	0.98	0.75	3.08	3.55	3.85	4.32	0.29	0.13	0.10	0.07
AR113Δ*Lp*_2739	1.57	1.21	–	–	2.92	3.57	–	–	0.23	0.15	–	–
AR113Δ*Lp*_2792	1.62	1.15	0.84	0.71	2.74	3.59	4.36	4.01	0.24	0.15	0.07	0.07
AR113Δ*Lp*_2805	1.53	1.38	2.75	0.20	3.41	3.84	–	–	0.22	0.16	–	–
AR113Δ*Lp*_1431&2792	1.37	1.07	0.77	0.68	2.27	3.50	4.07	3.84	0.31	0.14	0.07	0.05
AR113Δ*Lp*_1431Δ*Lp*_2233Δ*Lp*_2792	1.32	1.17	0.83	0.70	2.31	3.78	4.43	4.04	0.25	0.14	0.07	0.06

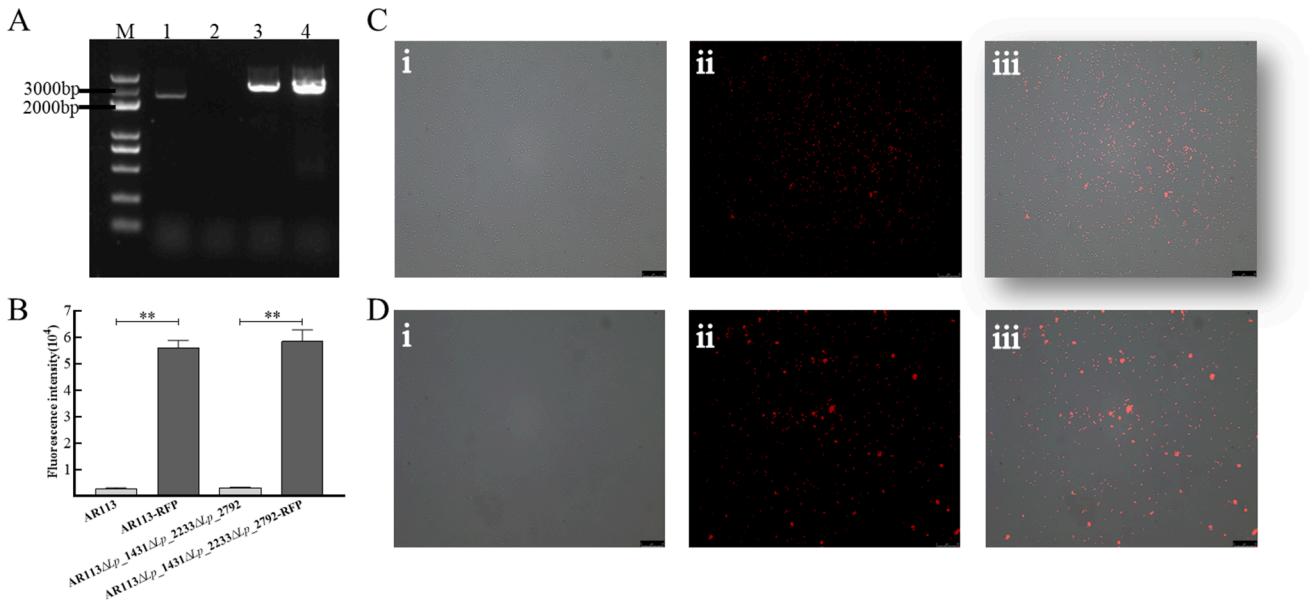

Fig. 4. A: M:5000bp Marker, Line1: positive control, Line2: negative control, Line3:AR113-RFP, Line4: AR113△*Lp*_1431△*Lp*_ 2233△*Lp*_2792-RFP. I: Fluorescence intensity measurement of strains. J: Bright field image, I: Fluorescence observation image, L: Overlay images of bright field and fluorescence.

assays and protein heterologous expression (Buntin et al., 2017, Gross et al., 2010; Holst et al., 2019; Kaushik et al., 2009; Singh et al., 2018), and these approaches that are inadequate in considering the global functional genetic aspects of probiotics. The genes involved in this study (*Lp*_0819, *Lp*_1080, *Lp*_1431, *Lp*_2233, *Lp*_2739, *Lp*_2792, *Lp*_2805) were compared with those in the *L. plantarum* WCFS1 genome (in order: lp_0964, lp_1229, lp_1643, lp_2486, lp_3059, lp_3114, lp_3127, and were found to be more than 97% homologous in percentage identity.

Based on the results of adhesion assays with HT-29 cells, there was no significant difference in the number of adhesions to cells between the single knockout strain and the wild-type strain. Therefore, we hypothesized that the possible reason is the existence of genetic complementation, identified and analyzed the domains organization of these mucins according to the NCBI Conserved Domain Database (CDD) (Marchler-Bauer et al., 2015). MucBP family proteins play an important role in the mucus adhesion process between lactic acid bacteria and their hosts, and the LPXTG anchoring motifs can assist in the accurate localization and assembly of exogenous proteins to the surface of the bacterial body (Roos, et al., 2002; Boekhorst et al., 2006). The experimental results confirmed that the simultaneous knockout of *Lp*_1431, *Lp*_2792 and *Lp*_2233 genes significantly decreased the adhesion ability of the strain compared to the wild-type strain.

The auto-aggregation, hydrophobicity, co-aggregation and adhesion to HT-29 cells of all of the strains were evaluated. The hydrophobicity of the strains (89.0% ~ 98.00%, except the wild-type) was greater than that of 15 *L. plantarum* strains in previously studied (45.54–6.67%) (Tuo et al., 2013), and the auto-aggregation of those strains (23.86–33.57%) was similar to the values obtained in this study (11.29–32.14%). In terms of co-aggregation, the co-aggregation values of the strains in our study (11.36–28.33%) were lower than that of *L. paracasei* subsp. *paracasei BGSJ2-8* (45%) (Nikolic et al., 2010). In terms of adhesion to HT-29 cells, compared to AR113, the mucin gene multiple knockout strain (AR113Δ*Lp*_1431Δ*Lp*_2233Δ*Lp*_2792) was significantly different from the wild-type strain in terms of adhesion to cells ($p < 0.01$), whereas knockout *Lp*_1080 (mannose-specific linkage) did not alter the adhesion ability of the strain, in agreement with the findings of Buntin (Buntin et al., 2017). Based on Pearson correlation analysis, the bacteria auto-aggregation and co-aggregation did not correlate with their adhesive ability, while there was a negative correlation between the hydrophobicity and adhesive ability of *L. plantarum* (r = −0.30). Thus, hydrophobicity can be used as an indicator to screen better probiotics (Xu et al., 2009). It has also been suggested that the adhesive capacity of bacteria cannot be described by hydrophobicity alone, but should be combined with other surface properties (e.g., auto-aggregation and co-aggregation) to assess the adhesive ability of bacteria (Tuo et al., 2013; García-Cayuela et al., 2014; Vlková et al., 2008).

A better probiotic strain must be tolerant to gastric acid and bile salts as they passed through the stomach and proximal small intestine to ensure that they reached their intestinal site in a viable state (Jovanović et al., 2015; Min et al., 2005). In our study, the knockout genes did not alter the acid tolerance of the strains, and in bile salt tolerance assays, different knockout strains differ in their ability to tolerate different concentrations of bile salts. Under normal physiological conditions, bile salt concentrations in our intestine range from 0.05% w/v to 2% w/v, and bile salt levels of 0.3% w/v are often used to assess the ability of strains to tolerate bile salts (Begley, et al., 2005; Ruiz, et al., 2013). At low concentrations of bile salts (<0.3% w/v) *Lactobacillus* has a self-protective mechanism of tolerance and adaptation (Bustos et al., 2012). For example, bile salt hydrolases in *Lactobacillus* can convert primary bile salts, which are more toxic to bacteria, into secondary bile salts, which are less toxic, and can also respond to bile salt stress by altering the expression of antioxidant enzyme genes, ion pump protein genes, and sugar paralogous genes (Bron et al., 2004). Most knockout strains in this study grew indistinguishably from wild-type strains at bile salt concentrations of 0.2% w/v. In contrast, AR113Δ*Lp*_1080, AR113Δ*Lp*_2739 and AR113Δ*Lp*_2805 showed stagnant growth at high bile salt concentrations (0.4% w/v). Similarly, Most (31 of 47) *Lactobacillus* strains examined did not replicate in broth supplemented with 0.3% oxgall and growth of the remaining strains was delayed (Jacobsen et al., 1999). The main reason is that high concentrations of bile salts can alter the permeability of bacterial cell membranes, causing damage or even death of bacteria and a decrease in bacterial biomass (Wang et al., 2011). It has been shown that the expression of mucin genes correlates with bacterial tolerance to bile salts. In a previous study, the expression of mucin (lp_1643) in *L.plantarum* WCFS1 decreased more than 2.5-fold under bile salt stress conditions (Bron et al., 2010). Similarly, the expression of surface adhesion protein (elongation factor-tu, EF-TU) was reduced in mutant strains (bile salt resistant) under 0.2% w/v bile salt

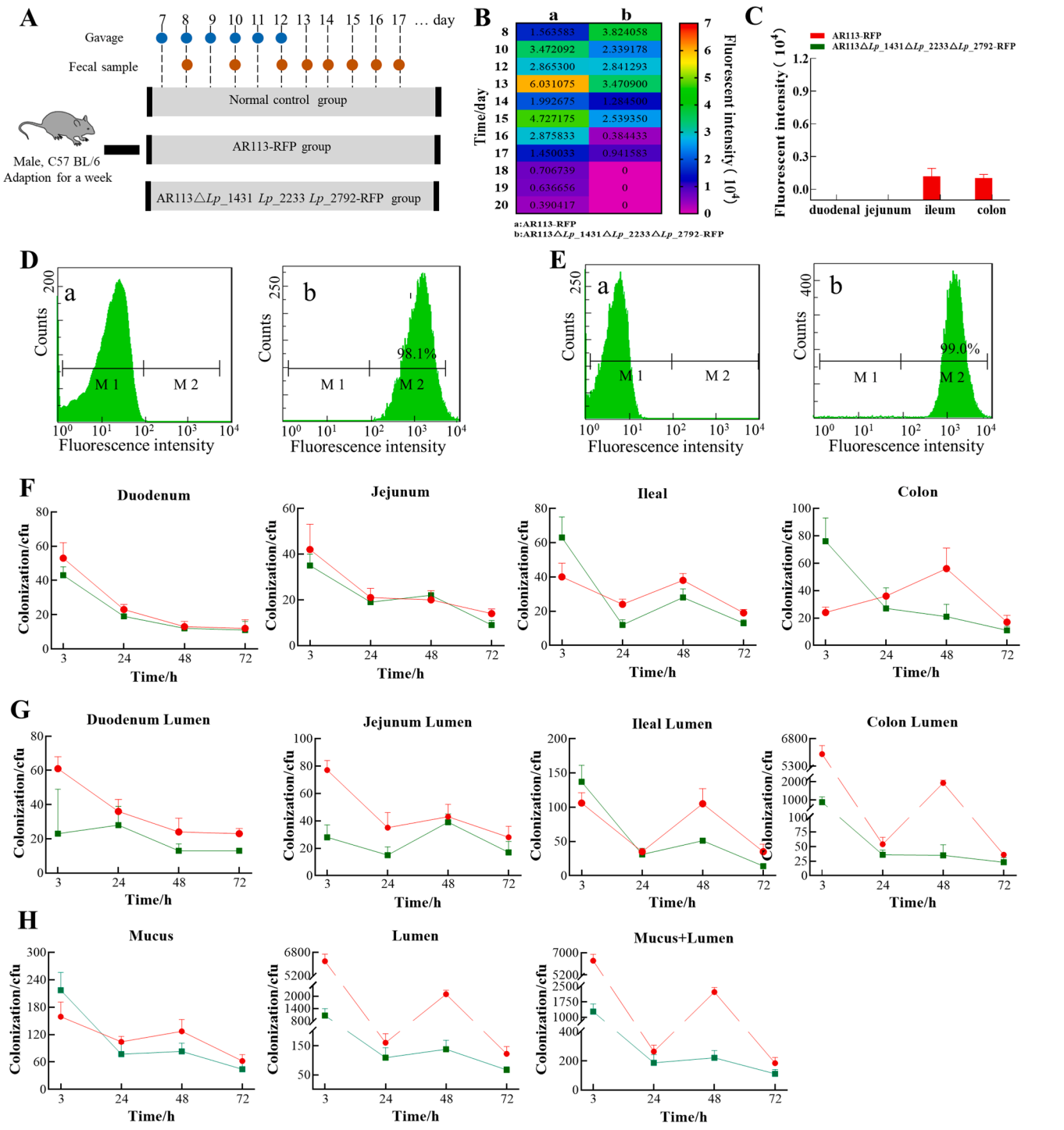

Fig. 5. *L. plantarum* in vivo colonization experiment. A; In vivo colonization experimental design. B-C: Fluorescence intensity of in feces with time. D-E: FCM of cFDA-SE-labeled strains before (a) and after (b), A, B represent AR113-RFP, AR113△*Lp*_1431△*Lp*_ 2233△*Lp*_2792-RFP, respectively. F-E: changes in the number of adhesion in the intestinal mucus, and lumen at different sites with time, respectively. H: changes in the number of attachments in intestinal mucus and lumen with time. Data are represented as means ± standard deviations, each experiment was repeated in triplicate (n = 3).

conditions compared to wild-type strains (Burns et al., 2010). Furthermore, the expression of mucin genes is different in different concentrations of bile salts. s-layer protein-encoding gene (*slpA*) expression is increased in 0.01%-0.05% of bile and decreased in 0.1% of bile (Khaleghi et al., 2010). Mucins act as a component of the cell wall (Kleerebezem et al., 2009; Sanchez, et al., 2010), and mucin genes are knocked out, theoretically, the cell wall is disrupted and bacteria are more vulnerable at bile salt concentrations. but the bacterial response to bile salts is a complex series of stress responses, the mechanisms of which need to be further explored.

Although the colonization potential of bacteria in the intestine has been explored by in vitro experiments, it is not possible to simulate the real in vivo environment. Therefore, it is necessary to further investigate the colonization and distribution of bacteria in vivo, however, it is

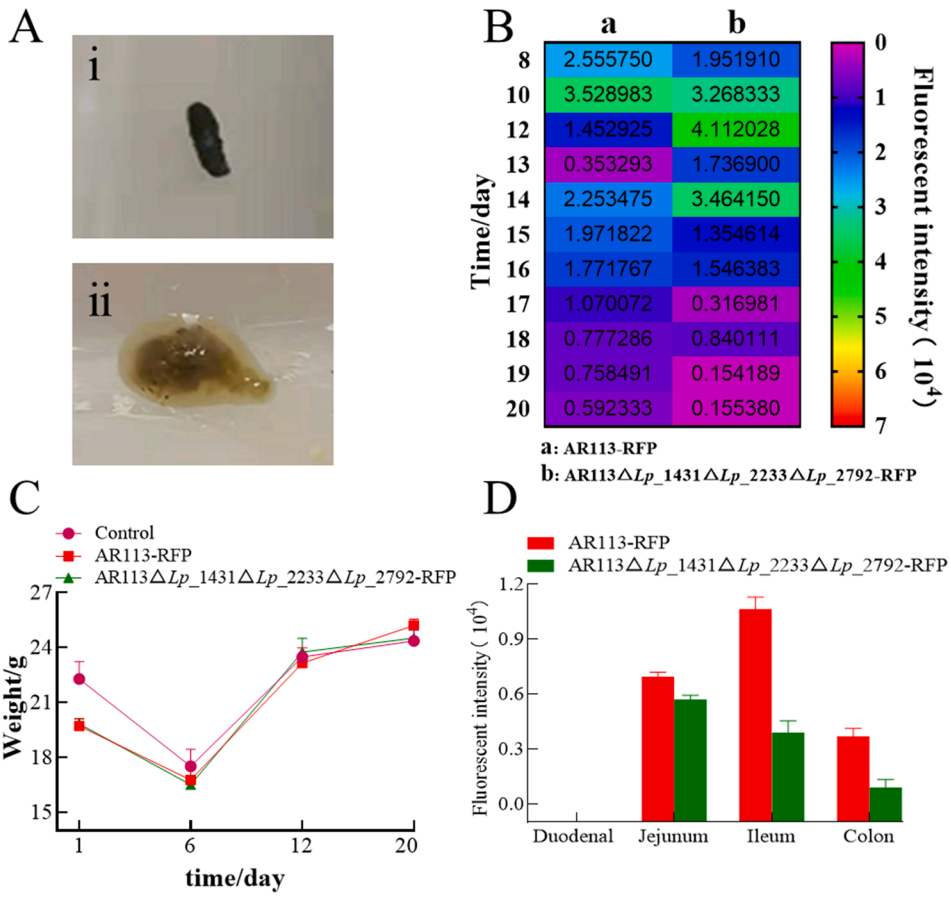

Fig. 6. Fluorescence intensity of *L. plantarum* in feces with time. A: a and b represent normal drinking water and PEG-treated mice, respectively. B: Weight change of mice before and after PEG treatment. C-D: fluorescence intensity of the strains in fecal after PEG treatment with time. Data are represented as means ± standard deviations, each experiment was repeated in triplicate (n = 3).

particularly important to trace the ingested bacteria. Previous researchers traced probiotics in vivo by using fluorescent reporter genes to assess the potential colonization in vivo (Russo et al., 2015; Wang et al., 2011; Cui et al., 2020). The disadvantage of this approach is that the fluorescent reporter plasmids are easily lost and interfere with the assay results.

In our work, on the one hand, the RFP gene was inserted into *L. plantarum* genome using CRISPR-Cas9 gene editing technology as a reporter system for probing bacterial colonization in vivo without affecting the bacterial growth. In the in vivo experiment, it was found that the knockout of the *Lp*_1431 *Lp*_2233 *Lp*_2792 genes significantly shortened the colonization time in the intestine (14 days to 11 days) (Fig. 5 B). Interestingly, the fluorescence intensity of the two strains showed a strong increase the day after the end of gavage. On the other hand, We further explored the colonization of *L. plantarum* in the mouse intestine by using cFDA-SE to label AR113-RFP, AR113Δ*Lp*_1431Δ*Lp*_2233Δ*Lp*_2792-RFP. After a single oral dose, a sharp increase in the number of strains was found, which demonstrated that the strains were able to multiply in vivo. In addition, the number of wild-type strain was higher than the number of knockout strains, indicating that the weakened adhesion ability of the knockout strain contributed significantly to their reduced numbers. The colonization sites of *L. plantarum* in the intestine were mainly in the colon, which is consistent with the Salomé-Desnoulez study (Salomé-Desnoulez et al.,2021).

Each site in the host gut is occupied by native microbiota; therefore, it is not easy for foreign strains to colonize the host gut (Marco et al.,2009; Zhou et al.,2019; Litvak and Baumler, 2019). The addition of 25% PEG to the drinking water of mice was able to simplify the abundance of intestinal native microbiota, and the method also did not cause intestinal epithelial damage in previous studies (Cabral et al., 2019). Therefore, this study was used to investigate the effect of host intestinal environment on the colonization of *L. plantarum* in vivo. The results revealed that the knockout strain had increased colonization time in the intestine of mice in the treated group compared to the intestinal environment without PEG treatment, and distributed in the duodenum, jejunum, ileum and colon. This suggests that the genetic background of the host has an important role in the in vivo colonization of *L. plantarum*.

5. Conclusions

In conclusion, previous studies on the effect of mucin genes on the colonization ability of bacterial strains mainly focused on the assessment of in vitro adhesion ability, and were not investigated by means of gene knockout. In our study, we assessed the ability of mucins genes to affect the colonization of *L. plantarum* in vitro and in vivo by means of gene knockouts, and found that mannose-specific adhesion was not always essential for adhesion to the host intestinal mucus. Notably, these results indicate that both mucins and the host intestinal environment affect the intestinal colonization of *L. plantarum*. However, the mechanism of colonization remains to be further investigated and elucidated.

The authors declare that they have no known competing financial interests or personal relationships that could have appeared to influence the work reported in this paper.

Funding

This study was funded by National Natural Science Foundation of China (No. 31972056) and National Science Foundation for Distinguished Young Scholars of China (No. 32025029).

CRediT authorship contribution statement

Wenfei Qin: Conceptualization, Methodology, Validation, Writing – original draft, Writing – review & editing. **Yongjun Xia:** Validation, Investigation. **Zhiqiang Xiong:** Data curation, Resources. **Xin Song:** Writing – review & editing. **Lianzhong Ai:** Conceptualization, Writing – original draft, Writing – review & editing, Supervision, Project administration, Funding acquisition. **Guangqiang Wang:** Supervision, Writing – original draft, Writing – review & editing, Supervision, Project administration, Funding acquisition.

Declaration of Competing Interest

The authors declare that they have no known competing financial interests or personal relationships that could have appeared to influence the work reported in this paper.

Appendix A. Supplementary material

Supplementary data to this article can be found online at https://doi.org/10.1016/j.foodres.2022.111382.

References

Begley, M., Gahan, C. G., & Hill, C. (2005). The interaction between bacteria and bile. *FEMS Microbiology Reviews, 29*(4), 625–651. https://doi.org/10.1016/j.femsre.2004.09.003

Boekhorst, J., Helmer, Q., Kleerebezem, M., & Siezen, R. J. (2006). Comparative analysis of proteins with a mucus-binding domain found exclusively in lactic acid bacteria. *Microbiology, 152*(1), 273–280. https://doi.org/10.1099/mic.0.28415-0

Roos, S., Jonsson, H. (2002). A high-molecular-mass cell-surface protein from *lactobacillus reuteri* 1063 adheres to mucus components. *Microbiology*, 148(2), 433-442. https://doi. org/10.1099/00221287-148-2-433.

Bron, P. A., Marco, M., Hoffer, S. M., Van Mullekom, E., De Vos, W. M., & Kleerebezem, M. (2004). Genetic characterization of the bile salt response in lactobacillus plantarum and analysis of responsive promoters in vitro and in situ in the gastrointestinal tract. *Journal of Bacteriology*. https://doi.org/10.1128/JB.186.23.7829-7835.2004

Bron, P. A., Molenaar, D., Vos, W. M. D., & Kleerebezem, M. (2010). DNA micro-array-based identification of bile-responsive genes in lactobacillus plantarum. *Journal of Applied Microbiology, 100*(4), 728–738. https://doi.org/10.1111/j.1365-2672.2006.02891.x

Buntin, N., de Vos, W. M., & Hongpattarakere, T. (2017). Variation of mucin adhesion, cell surface characteristics, and molecular mechanisms among *Lactobacillus plantarum* isolated from different habitats. *Applied Microbiology & Biotechnology, 101*(2), 7663–7674. https://doi.org/10.1007/s00253-017-8482-3

Burns P, Sánchez B., Vinderola G., Ruas-Madiedo P., Ruiz L., Margolles A., Reinheimer J., &de los Reyes-Gavilán CG. (2010). Inside the adaptation process of lactobacillus delbrueckii subsp. lactis to bile. *International Journal of Food Microbiology*, 142(1-2), 132-141. https://doi.org/10.1016/j.ijfoodmicro.2010.06.013.

Bustos, A. Y., Saavedra, L., Valdez, G. F. D., Raya, R. R., & Taranto, M. P. (2012). Relationship between bile salt hydrolase activity, changes in the internal ph and tolerance to bile acids in lactic acid bacteria. *Biotechnology Letters, 34*(8), 1511–1518. https://doi.org/10.1007/s10529-012-0932-5

Cabral, D. J., Penumutchu, S., Reinhart, E. M., Zhang, C., Korry, B. J., Wurster, J. I., … Belenky, P. (2019). Microbial metabolism modulates antibiotic susceptibility within the murine gut microbiome. *Cell Metabolism, 30*(4), 800–823. https://doi.org/10.1016/j.cmet.2019.08.020

Carasi, P., Ambrosis, N. M., De Antoni, G. L., Bressollier, P., Urdaci, M., & Serradell, M. (2014). Adhesion properties of potentially probiotic *Lactobacillus kefiri* to gastrointestinal mucus. *The Journal of dairy research, 81*(1), 1–8. https://doi.org/10.1017/S0022029913000526

Collado, M. C., Meriluoto, J., & Salminen, S. (2007). Adhesion and aggregation properties of probiotic and pathogen strains. *European Food Research & Technology, 226*(5), 1065–1073. https://doi.org/10.1007/s00217-007-0632-x

Cui, S. M., Chen, C. L., Gu, J. Y., Mao, B. Y., Zhang, H., Zhao, J. X., & Chen, W. (2020). Tracing *Lactobacillus plantarum* within the intestinal tract of mice: Green fluorescent protein-based fluorescent tagging. *Journal of the Science of Food and Agriculture, 101*(5), 1758–1766. https://doi.org/10.1002/jsfa.10789

Fornelos, N., Franzosa, E. A., Bishai, J., Annand, J. W., Oka, A., Lloyd-Price, J., … Xavier, R. J. (2020). Growth effects of N-acylethanolamines on gut bacteria reflect altered bacterial abundances in inflammatory bowel disease. *Nature Microbiology, 5*(3), 486–497. https://doi.org/10.1038/s41564-019-0655-7

Ganesh, B.P., Hall, A., Ayyaswamy, S., Nelson, J.W., Fultz, R., Major, A., Haag, A., Esparza, M., Lugo, M., Venable, S., Whary, M., Fox, J.G., &Versalovic, J. (2018). Diacylglycerol kinase synthesized by commensal *Lactobacillus reuteri* diminishes protein kinase C phosphorylation and histamine-mediated signaling in the mammalian intestinal epithelium. Mucosal Immunology. *Mucosal Immunology*, 11(2),380-393. https://doi.org/10.1038/mi.2017.58.

García-Cayuela, T., Korany, A. M., Bustos, I., Gómez de Cadiñanos, L. P., Requena, T., Peláez, C., & Martínez-Cuesta, M. C. (2014). Adhesion abilities of dairy *Lactobacillus plantarum* strains showing an aggregation phenotype. *Food Research International, 57*, 44–50. https://doi.org/10.1016/j.foodres.2014.01.010

Gross, G., Snel, J., Boekhorst, J., Smits, M. A., & Kleerebezem, M. (2010). Biodiversity of mannose-specific adhesion in *Lactobacillus plantarum* revisited: Strain-specific domain composition of the mannose-adhesin. *Benef Microbes, 1*, 61–66. https://doi.org/10.3920/BM2008.1006

Hamadi, F., Latrache, H., Zahir, H., Abed, S. E., Ellouali, M., & Saad, I. K. (2012). The relation between the surface chemical composition of escherichia coli and their electron donor/electron acceptor (acid-base) properties. *Research Journal of Microbiology, 7*(1), 32–40. https://doi.org/10.3923/jm.2012.32.40

Holst, B., Glenting, J., Holmstrom, K., Israelsen, H., Vrang, A., Antonsson, M., … Madsen, S. M. (2019). Molecular switch controlling expression of the mannose-specific adhesin, Msa, in *Lactobacillus plantarum*. *Applied and Environmental Microbiology, 85*, e02954–e03018. https://doi.org/10.1128/AEM.02954-18

Huang, H., Song, X., & Yang, S. (2019). Development of a RecE/T-assisted CRISPR-Cas9 toolbox for *Lactobacillus*. *Biotechnology Journal, 14*(7), 1800690. https://doi.org/10.1002/biot.201800690

Jacobsen CN, Rosenfeldt Nielsen V, Hayford AE, Møller PL, Michaelsen KF, Paerregaard A, Sandström B, Tvede M, Jakobsen M. (1999). Screening of probiotic activities of forty-seven strains of Lactobacillus spp. by in vitro techniques and evaluation of the colonization ability of five selected strains in humans. *Appl Environ Microbiol*. 1999 Nov;65(11):4949-56. https://doi.org/10.1128/AEM.65.11.4949-4956.1999.

Jang, S. E., Han, M. J., Kim, S. Y., & Kim, D. H. (2014). *Lactobacillus plantarum* CLP-0611 ameliorates colitis in mice by polarizing M1 to M2-like macrophages. *International Immunopharmacology, 21*(1), 186–192. https://doi.org/10.1016/j.intimp.2014.04.021

Jovanović, J. N., Nikolić, B., Šeatović, S., Zavišić, G., Mitić-Ćulafić, D., Vuković-Gačić, B., & Knežević-Vukčević, J. (2015). Characterization of some potentially probiotic *Lactobacillus* strains of human origin. *Food Science & Biotechnology, 24*(5), 1781–1788. https://doi.org/10.1007/s10068-015-0232-7

Kaushik, J. K., Kumar, A., Duary, R. K., Mohanty, A. K., Grover, S., & Batish, V. K. (2009). Functional and probiotic attributes of an indigenous isolate of *Lactobacillus plantarum*. *PLoS ONE, 4*, Article e8099. https://doi.org/10.1371/journal.pone.0008099

Khaleghi, M., Kermanshahi, R. K., Yaghoobi, M. M., Zarkesh-Esfahani, S. H., & Baghizadeh, A. (2010). Assessment of bile salt effects on s-layer production, slp gene expression and some physicochemical properties of *Lactobacillus acidophilus ATCC* 4356. *Journal of Microbiology and Biotechnology, 20*(4), 749–756. https://doi.org/10.4014/jmb.0906.06050

Kleerebezem, M., & Vaughan, E. E. (2009). Probiotic and gut lactobacilli and bifidobacteria: Molecular approaches to study diversity and activity. *Annual Review of Microbiology, 63*(1), 269–290. https://doi.org/10.1146/annurev.micro.091208.073341

Lee, Y. K., Ho, P. S., Low, C. S., Arvilommi, H., & Salminen, S. (2004). Permanent colonization by *Lactobacillus casei* is hindered by the low rate of cell division in mouse gut. *Applied and Environmental Microbiology, 70*(2), 670–674. https://doi.org/10.1128/AEM.70.2.670674.20 04

Lin, X., Xia, Y., Yang, Y., Wang, G., & Ai, L. (2020). Probiotic characteristics of lactobacillus plantarum ar113 and its molecular mechanism of antioxidant. *LWT – Food Science and Technology, 126*, Article 109278. https://doi.org/10.1016/j.lwt.2020.109278

Litvak, Y., & Baumler, A. J. (2019). The founder hypothesis: A basis for microbiota resistance, diversity in taxa carriage, and colonization resistance against pathogens. *PLoS Pathogens, 15*(2), 1007563. https://doi.org/10.1371/journal.ppat.1007563

Marchler-Bauer, A., Derbyshire, M. K., Gonzales, N. R., Lu, S., Chitsaz, F., Geer, L. Y., … Bryant, S. H. (2015). CDD: NCBI's conserved domain database. *Nucleic Acids Research, 43*, 222–226. https://doi.org/10.1093/nar/gku1221

Marco, M. L., Bongers, R. S., de Vos, W. M., & Kleerebezem, M. (2007). Spatial and temporal expression of *Lactobacillus plantarum* genes in the gastrointestinal tracts of mice. *Applied and Environmental Microbiology, 73*(1), 124–132. https://doi.org/10.1128/AEM.01475-06

Marco, M. L., Peters, T. H. F., Bongers, R. S., Molenaar, D., van Hemert, S., Gordon, J. I., & Kleerebezem, M. (2009). Lifestyle of *Lactobacillus plantarum* in the mouse caecum. *Environmental Microbiology, 11*(10), 2747–2757. https://doi.org/10.1111/j.1462-2920.2009.02001.x

Matz, M. V., Fradkov, A. F., Labas, Y. A., Savitsky, A. P., & Lukyanov, S. A. (1999). Erratum: Fluorescent proteins from nonbioluminescent Anthozoa species. *Nature Biotechnology, 17*(10), 969–973. https://doi.org/10.1038/70787

Min, T. L., & Shah, N. P. (2005). Acid and bile tolerance and the cholesterol removal ability of bifidobacteria strains. *Bioscience of Microbiota Food & Health, 24*(1), 1–10. https://doi.org/10.12938/bifidus.24.1.

Muñoz-Provencio, D., Llopis, M., Antolín, M., de Torres, I., Guarner, F., Perez-Martinez, G., & Monedero, V. (2009). Adhesion properties of *Lactobacillus casei* strains to resected intestinal fragments and components of the extracellular matrix. *Archives of Microbiology, 191*(2), 153–156. https://doi.org/10.1007/s00203-008-0436-9

Nikolic, M., Jovcic, B., Kojic, M., & Topisirovic, L. (2010). Surface properties of *Lactobacillus* and *Leuconostoc* isolates from homemade cheeses showing auto-aggregation ability. *European Food Research&Technology, 231*(6), 925–931. https://doi.org/10.1007/s00217-010-1344-1

Ruiz, L., Margolles, A., & Sánchez, B. (2013). Bile resistance mechanisms in Lactobacillus and Bifidobacterium. *Front Microbiol, 4*, 396. https://doi.org/10.3389/fmicb.2013.00396

Russo, P., Iturria, I., Mohedano, M. L., Caggianiello, G., Rainieri, S., Fiocco, D., … Spano, G. (2015). Zebrafish gut colonization by mCherry-labelled lactic acid bacteria. *Applied Microbiology&Biotechnology, 99*(8), 3479–3490. https://doi.org/10.1007/s 00253-014-6351-x

Salomé-Desnoulez, S., Poiret, S., Foligné, B., Muharram, G., Peucelle, V., Lafont, F., & Daniel, C. (2021). Persistence and dynamics of fluorescent *Lactobacillus plantarum* in the healthy versus inflamed gut. *Gut Microbes, 13*(1), 1–16. https://doi.org/10.1080/19490976.2021. 1897374

Sanchez, B., Urdaci, M. C., & Margolles, A. (2010). Extracellular proteins secreted by probiotic bacteria as mediators of effects that promote mucosa-bacteria interactions. *Microbiology, 156*(11), 3232–3242. https://doi.org/10.1099/mic.0.044057-0

Satish Kumar, C. S. V., Kondal Reddy, K., Reddy, A. G., Vinoth, A., Ch, S. R. C., Boobalan, G., & Rao, G. S. (2015). Protective effect of *Lactobacillus plantarum* 21, a probiotic on trinitrobenzenesulfonic acid-induced ulcerative colitis in rats. *International Immunopharmacology, 25*(2), 504–510. https://doi.org/10.1016/j.intimp.2015.02.026

Seddik, H. A., Bendali, F., Gancel, F., Fliss, I., Spano, G., & Drider, D. (2017). *Lactobacillus plantarum* and its probiotic and food potentialities. *Probiotics & Antimicrobial Proteins, 9*(2), 111–122. https://doi.org/10.1007/s12602-017-9264-z

Singh, K. S., Kumar, S., Mohanty, A. K., Grover, S., & Kaushik, J. K. (2018). Mechanistic insights into the host-microbe interaction and pathogen exclusion mediated by the mucus-binding protein of *Lactobacillus plantarum*. *Scientific Reports, 8*, 14198. https://doi.org/10.1038/s41598-018-32417-y

Tuo, Y. F., Yu, H. L., Ai, L. Z., Wu, Z. G., Guo, B. G., & Chen, W. (2013). Aggregation and adhesion properties of 22 *Lactobacillus* strains. *Journal of Dairy Science, 96*(7), 4252–4257. https://doi.org/10.3168/jds.2013-6547

Tropini, C., Moss, E. L., Merrill, B. D., Ng, K. M., Higginbottom, S. K., Casavant, E. P., … Sonnenburg, J. L. (2018). Transient osmotic perturbation causes long-term alteration to the gut microbiota. *Cell, 173*(7), 1742–1754. https://doi.org/10.1016/j.cell.2018.05.008

Vlková, E., Rada, V., Šmehilová, M., &Killer. J. (2008). Auto-aggregation and co-aggregation ability in *bifidobacteria* and *clostridia. Folia Microbiologica*, 53(3), 263-269. https://doi.or g/10.1007/s12223-008-0040-z.

Wang, Y., Xu, N., Xi, A., Ahmed, Z., Zhang, B., & Bai, X. (2009). Effects of *Lactobacillus plantarum* MA2 isolated from Tibet kefir on lipid metabolism and intestinal microflora of rats fed on high-cholesterol diet. *Applied Microbiology & Biotechnology, 84*(2), 341–347. https://doi.org/10.1007/s00253-009-2012-x

Wang, Y. P., Wang, J. G., & Dai, W. L. (2011). Use of GFP to trace the colonization of *Lactococcus lactis* WH-C1 in the gastrointestinal tract of mice. *Journal of Microbiological Methods, 86*(3), 390–392. https://doi.org/10.1016/j.mimet.2011.06.009

Wang, G., Sheng, Y., An, H., Chen, S., & Hao, Y. (2011). Coexpression of bile salt hydrolase gene and catalase gene remarkably improves oxidative stress and bile salt resistance in lactobacillus casei. *Journal of Industrial Microbiology & Biotechnology, 38*(8), 985–990. https://doi.org/10.1007/s10295-010-0871-x

Wang, G. Q., Liu, Y. N., Lu, Z., Yang, Y. T., Xia, Y. G., Lai, P. F. H., & Ai, L. Z. (2019). The ameliorative effect of a *Lactobacillus* strain with good adhesion ability against dextran sulfate sodium-induced murine colitis. *Food & Function, 10*(1), 397–409. https://doi.org/10.1039/c8fo0 1453a

Xu, H., Jeong, H. S., Lee, H. Y., & Ahn, J. (2009). Assessment of cell surface properties and adhesion potential of selected probiotic strains. *Letters in Applied Microbiology, 49*(4), 434–442. https://doi.org/10.1111/j.1472-765X.2009.02684.x

Zheng, J., Wittouck, S., Salvetti, E., Franz, C., Harris, H. M. B., Mattarelli, P., … Lebeer, S. (2020). A taxonomic note on the genus *Lactobacillus*: Description of 23 novel genera, emended description of the genus *Lactobacillus Beijerinck* 1901, and union of *Lactobacillaceae* and *Leuconostocaceae*. *International Journal of Systematic and Evolutionary Microbiology, 70*(4), 2782–2858. https://doi.org/10.1099/ijsem.0.004107

Zhou, W., Chow, K. H., Fleming, E., & Oh, J. (2019). Selective colonization ability of humanfecal microbes in different mouse gut environments. *The ISME Journal, 13*(3), 805–823. https://doi.org/10.1038/s41396-018-0312-9